

Spontaneous interlayer superfluidity in bilayer systems of cold polar molecules

Roman M. Lutchyn,^{1,2,*} Enrico Rossi,^{2,†} and S. Das Sarma^{1,2}

¹Joint Quantum Institute, Department of Physics, University of Maryland, College Park, Maryland 20742, USA

²Condensed Matter Theory Center, Department of Physics, University of Maryland, College Park, Maryland 20742, USA

(Received 11 July 2010; revised manuscript received 17 August 2010; published 13 December 2010)

Recent experimental progress in producing ultracold polar molecules with a net electric dipole moment opens up possibilities for realizing quantum phases governed by the long-range and anisotropic dipole-dipole interactions. In this work we predict the existence of experimentally observable broken-symmetry states with spontaneous interlayer coherence in cold polar molecule bilayers. These exotic states, which are manifestations of collective bilayer quantum entanglement, appear due to strong repulsive interlayer interactions and exhibit properties of superfluids, ferromagnets, and excitonic condensates.

DOI: [10.1103/PhysRevA.82.061604](https://doi.org/10.1103/PhysRevA.82.061604)

PACS number(s): 67.85.De, 05.30.Fk, 05.30.Rt

During the past decade we have observed the spectacular progress in the realization of various quantum phases using cold atoms. This progress has deepened our understanding of various phenomena such as BCS-BEC crossover of fermions [1] and superfluid-to-Mott-insulator phase transition of bosons in an optical lattice [2]. However, the variety of quantum phases that can be realized in cold-atom systems is limited by the short-range nature of the interparticle interactions. Recent progress in producing and manipulating heteronuclear polar molecules [3] provides an opportunity to realize a plethora of quantum phases of matter governed by long-range interactions [4]. This interesting prospect is made possible by the fact that polar molecules have large electric dipole moments associated with their rotational excitations, which lead to strong, long-range, and anisotropic dipole-dipole interactions. The interactions between such polar molecules can be tuned using dc and ac electric fields [5]. In what follows, we concentrate on one intriguing aspect of fermionic polar molecule systems—the possibility of realizing bilayer superfluidity (or, equivalently, bilayer XY ferromagnetism) with spontaneous interlayer coherence using interlayer molecular repulsion.

Because of the fermionic nature of the molecules even for the spinless fermion case considered here, the interaction has an exchange component in the layer (or pseudospin) index which drives the instability toward the bilayer superfluid phase. The dominant contribution to the exchange energy comes from the short distances (large momenta) where the interlayer dipolar interaction is repulsive. Thus, the collective bilayer state we predict arises from a repulsive interaction in sharp contrast to all other superfluid quantum phases discussed in cold atomic fermions where interparticle attraction leads to superfluidity. In the symmetry-broken interlayer coherent phase, the particle number in each layer becomes indeterminate in spite of the interlayer single-particle tunneling amplitude being almost zero. Such a state is very analogous to an excitonic superfluid in which excitons formed a quasiparticle in one layer “binding” to a quasihole in the other layer condense into a phase-coherent

state. Up to this date the clearest evidence for the realization of this type of exciton superfluid state has been observed in semiconductor bilayers in the quantum Hall (QH) regime, in which the layers are immersed in very high magnetic fields [6]. The unavoidable presence of disorder in solid-state systems as well as the nature of the measurement involving finite interlayer tunneling [7] cause complications in the pristine realization of the interlayer superfluid phase in QH bilayers. As a result, vortices and the Berezinskii-Kosterlitz-Thouless (BKT) transition, unambiguous signatures of the interlayer coherent state, have not been observed yet in solid-state QH systems. The predicted polar molecule bilayer superfluid phase should be more striking because of the lack of disorder in cold-atom systems, the tunability of the interaction strength, and the availability of experimental techniques allowing imaging of vortices [8]. Moreover, by adding an optical lattice potential in the xy plane it is possible to modify the single-particle dispersion of the particles and model various condensed-matter systems. For example, the bilayer cold-polar-molecule system with honeycomb lattice potential will mimic the bilayer graphene system. Thus, the realization of this interesting phase in cold-atom systems is of great importance for understanding the instabilities driving the bilayer superfluidity and in general the physics of exciton condensation.

Theoretical model. Our starting point is the Hamiltonian for fermionic polar molecules tightly confined along the z direction by the laser field as shown in Fig. 1(b). We consider two clouds of polar molecules separated by a distance l_z much larger than the confinement length w_z of the molecules within each layer. When the confinement length w_z is much larger than the size of the polar molecules, the rotational motion of the molecules is three-dimensional and is described by a three-dimensional rigid rotor Hamiltonian. Polar molecules have permanent electric dipole moment d , which couples to internal rotational degrees of freedom. The dipole moment leads to long-range interlayer and intralayer dipole-dipole interactions. The Hamiltonian of the polar molecules H reads ($\hbar = k_B = 1$) [5],

$$H = \sum_i \left(\frac{p_i^2}{2m} + B J_i^2 \right) + \sum_{ij} \frac{\mathbf{d}_i \cdot \mathbf{d}_j - 3(\mathbf{d}_i \cdot \hat{\mathbf{r}}_{ij})(\mathbf{d}_j \cdot \hat{\mathbf{r}}_{ij})}{2r_{ij}^3}, \quad (1)$$

*Present address: Microsoft Research, Station Q, Elings Hall, University of California, Santa Barbara, CA 93106, USA.

†Present address: Department of Physics, College of William and Mary, Williamsburg, VA 23187, USA.

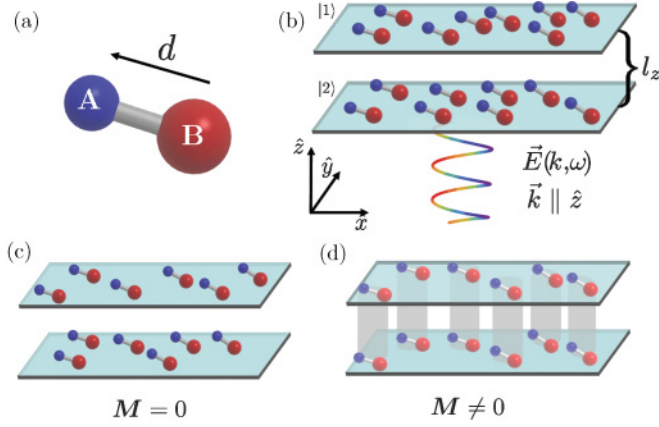


FIG. 1. (Color online) (a) Heteronuclear polar molecules AB with AB being $^{40}\text{K}^{87}\text{Rb}$, $^7\text{Li}^{40}\text{K}$, $^6\text{Li}^{133}\text{Cs}$. (b) Bilayer system of cold polar molecules in the presence of a circularly polarized ac electromagnetic field propagating along the z direction. Schematic picture of different phases in the bilayers system: normal (c) and pseudospin ferromagnetic (d).

where $\mathbf{p} = (p_x, p_y)$ is the center-of-mass momentum of a molecule with mass m , r_{ij} is the distance between two molecules, B is the effective rotational energy, and $\mathbf{J} = (J_x, J_y, J_z)$ is the angular momentum operator. The rotational eigenstates are $|J, M_J\rangle$ with J and M_J denoting the total internal angular momentum and its projection on the quantization axis, respectively.

The orientation of the dipole moments can be controlled with dc and ac electric fields Fig. 1(b) [5]. The transition dipole moment between the states with $J = 0$ and $J = 1$ is $d_t \equiv |\langle 0,0|\mathbf{d}|1, M_J\rangle| = d/\sqrt{3}$, with $M_J = 0, \pm 1$. A circularly polarized ac electric field $\mathbf{E}_{ac}(t)$ propagating along z direction [see Fig. 1(b)] drives transitions between the rotational states $|0,0\rangle$ and $|1,1\rangle$ with Rabi frequency $\Omega_R = d_t E_{ac}$. If the frequency of the field ω is close to the transition frequency $\omega_0 = 2B$ between the states $|0,0\rangle$ and $|1,1\rangle$ (i.e., the detuning $\Delta = \omega - \omega_0 \ll \omega_0$), the leading effect of the electric field is to mix these two states. Within the rotating wave approximation, the dressed states are given by $|\pm\rangle = \alpha_{\pm}|0,0\rangle \pm \alpha_{\mp}e^{-i\omega t}|1,1\rangle$, where $\alpha_{+} = -\Gamma/\sqrt{\Gamma^2 + \Omega_R^2}$, $\alpha_{-} = \Omega_R/\sqrt{\Gamma^2 + \Omega_R^2}$, and $2\Gamma = \Delta + \sqrt{\Delta^2 + 4\Omega_R^2}$ [5,9]. Polar molecules can be prepared in the internal state $|+\rangle_i$ by an adiabatic switching of the microwave field. In this case, the effective interaction between polar molecules $V_{\text{eff}}(r)$ is given by the dressed Born-Oppenheimer potential adiabatically connected to the state $|+\rangle_i \otimes |+\rangle_j$ (see Fig. 1 of the supplementary material [10]). At large distances the dipolar interaction can be obtained perturbatively by first calculating the effective dipole moment $\langle +|\mathbf{d}|+\rangle = d_{\text{eff}}(\cos \omega t, \sin \omega t, 0)$, with $d_{\text{eff}} = -\sqrt{2}\alpha_{+}\alpha_{-}d_t$. The time-averaged interaction between dipoles in layers λ and λ' takes the form

$$V_{\text{eff}}^{\lambda\lambda'}(\rho) = d_{\text{eff}}^2 \left(\frac{1}{(z_{\lambda\lambda'}^2 + \rho^2)^{\frac{3}{2}}} - \frac{3}{2} \frac{\rho^2}{(z_{\lambda\lambda'}^2 + \rho^2)^{\frac{5}{2}}} \right), \quad (2)$$

where $\rho = (x, y)$ is the two-dimensional coordinate and $z_{\lambda\lambda'} = l_z$ for $\lambda \neq \lambda'$ and zero otherwise. At short distances, when the

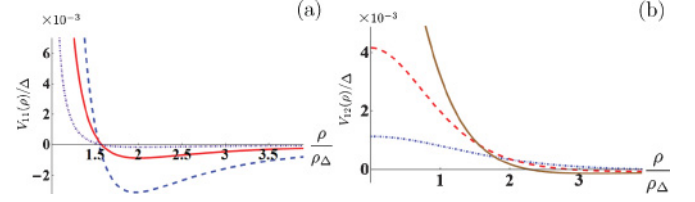


FIG. 2. (Color online) (a) Intralayer Born-Oppenheimer potential for polar molecules. The dashed (blue), solid (red), and dot-dashed (violet) lines correspond to $\Omega_R/\Delta = 1/4$, $\Omega_R/\Delta = 1/8$, and $\Omega_R/\Delta = 1/20$, respectively. (b) Interlayer Born-Oppenheimer potential for $\Omega_R/\Delta = 1/8$. The dash-dotted (blue), solid (red), and dashed (brown) lines correspond to $l_z/\rho_{\Delta} = 3, 2, 1.5$, $l_z/\rho_{\Delta} = 1.5$, respectively. For typical interparticle distances considered here the interlayer interaction is repulsive. Here $\Omega_R/\Delta = 1/8$ and $l_z/\rho_{\Delta} = 3$.

dipolar interaction energy is comparable with the detuning, the preceding perturbative treatment breaks down. In order to find the Born-Oppenheimer potential at short distances $\rho \leq \rho_{\Delta} \equiv (d_t^2/\Delta)^{\frac{1}{3}}$, it is necessary to account for all couplings between different angular momentum channels within the $J = 0, 1$ manifold [5]. The exact Born-Oppenheimer potentials are shown in Fig. 2. One can notice that the effective intralayer dipole-dipole interaction between polar molecules prepared in the state $|+\rangle$ becomes repulsive at $\rho \sim \rho_{\Delta}$ due to the presence of avoided crossings with other field-dressed levels [9]. For $^6\text{Li}^{133}\text{Cs}$ molecules, typical parameters are $d \approx 6.3$ D, $B \approx 6$ GHz, and $\Delta \approx 10$ MHz yielding the length scale $\rho_{\Delta} \approx 50$ nm that is much larger than the characteristic scale of dipole-dipole interactions $\rho_B = (d^2/B)^{1/3} \sim 1$ nm, which sets the short-range cutoff. Thus, for typical densities of polar molecules considered here, $n_0 \sim 10^7$ cm $^{-2}$, the ac electric field shields the molecules from short-range inelastic collisions and prevents the collapse of the system [5,9,11] (see supplementary document [10]).

Henceforth, we consider the dilute gases of polar molecules, where the interparticle distance is larger than ρ_{Δ} , that is, $l_z n_0^{-1/2} \gg \rho_{\Delta}$, and the interaction between particles is given by the dressed Born-Oppenheimer potentials shown in Fig. 2. In order to avoid unwanted inelastic collisions leading to the decay of the molecules in an s -wave channel, we assume the molecules to be spin-polarized. In this limit, the effective second-quantized Hamiltonian of the bilayer system takes the form

$$H = \sum_{k\lambda} [\varepsilon(k) - \mu_{\lambda}] c_{k\lambda}^{\dagger} c_{k\lambda} + \frac{1}{2} \sum_{q,k,k',\lambda,\lambda'} V_{\text{eff}}^{\lambda\lambda'}(q) c_{k+q\lambda}^{\dagger} c_{k'-q\lambda'}^{\dagger} c_{k'\lambda'} c_{k\lambda}, \quad (3)$$

where $c_{k\lambda}$ and $c_{k\lambda}^{\dagger}$ are the fermion creation and annihilation operators for a molecule with momentum \mathbf{k} in layer λ . The strength of the dipolar interactions can be characterized by the dimensionless parameter $r_s = d_{\text{eff}}^2 m \sqrt{n_0} / 2\pi$. As r_s is increased, the bilayer system becomes susceptible to various instabilities driven by the dipolar interactions. Here we concentrate on the instabilities induced by the interlayer interactions and neglect the instabilities induced by the

intralayer interactions (see supplementary material [10] for the justification of such approximations).

To understand the interlayer instability, it is convenient to draw an analogy with ferromagnetism and introduce pseudospin-1/2 operators $2\hat{m}_i = c_{i\lambda}^\dagger \sigma_{\lambda\lambda'} c_{i\lambda'}$. The spinors $|\uparrow\rangle$ and $|\downarrow\rangle$ represent the states in which molecules are in layer 1 or 2, respectively. When $l_z \gg k_F^{-1}$, with $k_F = \sqrt{4\pi n_0}$ being the Fermi momentum, the molecules in different layers are uncorrelated, and the many-body state of the system is given by

$$|\Psi_N\rangle = \prod_{k \leq k_F} c_{k1}^\dagger \prod_{k' \leq k_F} c_{k'2}^\dagger |0\rangle. \quad (4)$$

For equal densities in the layers $n_1 = n_2 = n_0$, the total magnetization \mathbf{M} is zero, $\mathbf{M} = \langle \Psi_N | \sum_i \hat{m}_i | \Psi_N \rangle = 0$, similar to paramagnets. The normal state $|\Psi_N\rangle$ minimizes the kinetic energy at the expense of the potential energy, which is at its maximum. When the interlayer distance becomes smaller than k_F^{-1} , the potential energy becomes large and at some point starts to dominate over the kinetic energy. In this case, the system favors the state in which fermions in different layers are correlated in a way that minimizes the interaction energy; that is, the molecule in layer 1 is coupled to a ‘‘hole’’ in layer 2. At the mean-field level such correlations are captured by an order parameter $\Delta_{12} \propto \langle c_{k1}^\dagger c_{k2} \rangle \neq 0$. Since the product wave function Ψ_N does not have such entanglement between the layers, the bilayer system should undergo a quantum phase transition as a function of the distance l_z or the strength of the dipole moment d_{eff} . The many-body wave function minimizing the interaction energy takes the form

$$|\Psi_{\text{FM}}\rangle = \prod_{k \leq \sqrt{2}k_F} \left(\frac{c_{k1}^\dagger + e^{i\varphi} c_{k2}^\dagger}{\sqrt{2}} \right) |0\rangle. \quad (5)$$

In this entangled state the state of the molecule is given by the coherent superposition of the amplitudes in different layers. Thus, even in the absence of tunneling, the molecule layer index becomes uncertain. Using the spin analogy, the state $|\Psi_{\text{FM}}\rangle$ has nonzero magnetization $\mathbf{M} = \langle \Psi_{\text{FM}} | \sum_i \hat{m}_i | \Psi_{\text{FM}} \rangle \neq 0$, with \mathbf{M} lying in the xy plane. Similar to superconductors, this ferromagnetic state $|\Psi_{\text{FM}}\rangle$ spontaneously breaks $U(1)$ symmetry and develops interlayer coherence. In this state the phase difference between different layers φ is well defined and the number of molecules in each layer fluctuates satisfying the uncertainty relations $\Delta m_z \Delta \varphi \geq 1/2$ [12] despite the absence of interlayer tunneling in Eq. (3).

The phase diagram between the two competing states—normal $|\Psi_N\rangle$ and pseudospin ferromagnetic $|\Psi_{\text{FM}}\rangle$ —can be obtained using variational mean-field calculation [13]. The total energy per area \mathcal{A} of the bilayer system in the normal phase is

$$\frac{E_N}{\mathcal{A}} = \frac{2\pi n_0^2}{m} \left(1 + r_s \frac{Z(2k_F \rho_\Delta)}{k_F \rho_\Delta \frac{d_{\text{eff}}^2}{d_l^2}} \right), \quad (6)$$

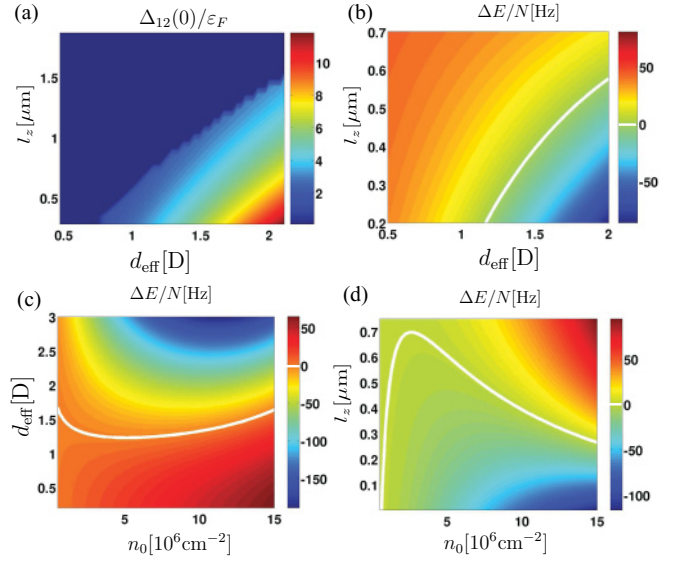


FIG. 3. (Color online) The dependence of $\Delta_{12}(0)$ and ΔE on l_z and d_{eff} is shown in (a) and (b), respectively. Here we used $\rho_\Delta = 50$ nm, $n_0 = 10^7$ cm $^{-2}$, and $m = 139m_p$, with m_p being the proton mass. The dependence of ΔE on n_0 and d_{eff} at fixed $l_z = 0.3$ μm and on n_0 and l_z at fixed $d_{\text{eff}} = 1.5$ D is plotted in (c) and (d), respectively.

where the dimensionless function $Z(a)$, which describes intralayer interaction, is defined as

$$Z(a) = \frac{32}{\sqrt{\pi}} \int_0^1 x dx f(x) \frac{[V_{\text{eff}}^{(11)}(0) - V_{\text{eff}}^{(11)}(ax)]}{\Delta \rho_\Delta^2}, \quad (7)$$

with $f(x) = \arccos(x) - x\sqrt{1-x^2}$. The momentum dependence of the intralayer interaction potential $V_{\text{eff}}^{(11)}(q)$ is shown in Fig. 1(b) of the supplementary material [10]. One can notice that the contribution of the interlayer Hartree term is zero here because $V_{\text{eff}}^{12}(q) = d_{\text{eff}}^2 \pi q e^{-ql_z}$ goes to zero as $q \rightarrow 0$. To calculate the energy of the system in the interlayer coherent state $|\Psi_{\text{FM}}\rangle$ we first introduce the order parameter

$$\Delta_{12}(k) = \frac{1}{2} \sum_q V_{12}(q) e^{-i\varphi} \langle c_1^\dagger(k+q) c_2(k+q) \rangle, \quad (8)$$

which takes into account interlayer correlations. The order parameter is obtained by numerically solving the preceding self-consistent equation, subject to the total particle number conservation constraint. Because of the dipolar nature of the interaction $\Delta_{12}(k)$ has momentum dispersion. The dependence of $\Delta_{12}(0)$ on d_{eff} and l_z obtained self-consistently is shown in Fig. 3(a). At the mean-field level, the Hamiltonian (3) can be diagonalized using a Bogoliubov transformation yielding the many-body variational wave function (5). For sufficiently large interactions the lowest energy state of the system corresponds to the pseudospin ferromagnetic state fully polarized in the xy plane [13] (see also supplementary material [10]). The total energy of the system per area in the interlayer coherent state is given by

$$\frac{E_{\text{FM}}}{\mathcal{A}} = \mathcal{E}_0 \left[1 - r_s F(\sqrt{8}k_F l_z) + \frac{r_s}{2} \frac{Z(\sqrt{8}k_F \rho_\Delta)}{k_F \rho_\Delta \frac{d_{\text{eff}}^2}{d_l^2}} \right], \quad (9)$$

where $\mathcal{E}_0 = 4\pi n_0^2/m$ and the function $F(a)$ describing the interlayer exchange contribution reads

$$F(a) = 32\sqrt{2\pi} \int_0^1 x^2 dx [\arccos(x) - x\sqrt{1-x^2}] e^{-ax}. \quad (10)$$

The energy difference between normal and ferromagnetic phase $\Delta E/\mathcal{A} = (E_{\text{FM}} - E_{\text{N}})/\mathcal{A}$ determines the mean-field phase diagram for the bilayers of polar molecules shown in Fig. 3.

The long-wavelength Hamiltonian describing the phase fluctuations is

$$H = \frac{1}{2} \int d^2\mathbf{r} \rho_s |\nabla\varphi|^2, \quad (11)$$

where ρ_s is the “spin stiffness,” which is the result of the loss of interaction energy due to the spatial variations of order parameter phase φ . The effective XY model defined by Eq. (11) undergoes BKT transition associated with unbinding of vortex pairs at the temperature $T_{\text{BKT}} \approx \pi\rho_s/2$. The “spin stiffness” can be calculated within linear response theory, which yields the result $\rho_s = n_0/2m$, similar to the one in superfluids. Thus, the BKT transition in the bilayer system of polar molecules occurs

at the temperature $T_{\text{BKT}} \approx \varepsilon_F/8$, with $\varepsilon_F = k_F^2/2m$, which for $n_0 \sim 10^7 \text{ cm}^{-2}$ corresponds to a temperature that should be accessible in the near future [14]. In the pseudospin ferromagnetic phase vortices are correlated in different layers, and the BKT transition in the bilayer system can be detected by imaging vortices using matter-wave heterodyning techniques [8].

In summary, we predict an unusual broken-symmetry phase with spontaneous interlayer coherence in a bilayer system of cold polar molecules. Our main findings, summarized in the phase diagram shown in Fig. 3, indicate that the experimental observation of such a phase requires low densities of cold polar molecules $n_0 \sim 10^7 \text{ cm}^{-2}$, realistic dipole moments $d_{\text{eff}} \sim 1\text{D}$, and reasonably low temperatures $T \sim 1 \text{ nK}$. Given that for these parameters the inelastic decay rate is small [10], the detection of this exotic many-body state should be within the experimental reach in the near future. The phase we predict is an interlayer entangled state, arising from the repulsive part of the dipolar interaction and exhibiting superfluidity (or, equivalently, XY pseudospin ferromagnetism) between the layers rather than within the layers.

We thank P.S. Julienne, I. Spielman, T. Porto, and, most particularly, D.-W. Wang, for helpful discussions. This work is supported by US-AFOSR-MURI and NSF-JQI-PFC.

-
- [1] M. Greiner, C. Regal, and D. Jin, *Nature (London)* **426**, 537 (2003); C. Chin *et al.*, *Science* **305**, 1128 (2004); M. Zwierlein *et al.*, *Nature (London)* **435**, 1047 (2005).
- [2] M. Greiner *et al.*, *Nature (London)* **415**, 39 (2002).
- [3] K. K. Ni *et al.*, *Science* **322**, 231 (2008); J. Deiglmayr *et al.*, *Phys. Rev. Lett.* **101**, 133004 (2008); F. Lang, K. Winkler, C. Strauss, R. Grimm, and J. HeckerDenschlag, *ibid.* **101**, 133005 (2008); S. Ospelkaus *et al.*, *Nat. Phys.* **4**, 622 (2008).
- [4] A. Micheli, G. K. Brennen, and P. Zoller, *Nat. Phys.* **2**, 341 (2006); D.-W. Wang, M. D. Lukin, and E. Demler, *Phys. Rev. Lett.* **97**, 180413 (2006); D.-W. Wang, *ibid.* **98**, 060403 (2007); H. P. Büchler *et al.*, *ibid.* **98**, 060404 (2007); C.-M. Chang, W. C. Shen, C. Y. Lai, P. Chen, and D. W. Wang, *Phys. Rev. A* **79**, 053630 (2009).
- [5] A. Micheli, G. Pupillo, H. P. Büchler, and P. Zoller, *Phys. Rev. A* **76**, 043604 (2007); A. V. Gorshkov *et al.*, *Phys. Rev. Lett.* **101**, 073201 (2008).
- [6] J. Eisenstein and A. MacDonald, *Nature (London)* **432**, 691 (2004).
- [7] I. B. Spielman, J. P. Eisenstein, L. N. Pfeiffer, and K. W. West, *Phys. Rev. Lett.* **84**, 5808 (2000).
- [8] Z. Hadzibabic *et al.*, *Nature (London)* **441**, 1118 (2006).
- [9] N. R. Cooper and G. V. Shlyapnikov, *Phys. Rev. Lett.* **103**, 155302 (2009).
- [10] See supplementary material at [<http://link.aps.org/supplemental/10.1103/PhysRevA.82.061604>].
- [11] R. Napolitano, J. Weiner, and P. S. Julienne, *Phys. Rev. A* **55**, 1191 (1997).
- [12] K. Moon *et al.*, *Phys. Rev. B* **51**, 5138 (1995).
- [13] L. Zheng, M. W. Ortalano, and S. Das Sarma, *Phys. Rev. B* **55**, 4506 (1997).
- [14] J. Ye (private communication).